JHEP PROCEEDINGS

International Europhysics Conference on HEP

Extension of the F_2 Structure Function Measurement towards low x and Q^2.

Arnulf Quadt *

Physikalisches Institut, Bonn University
Nußallee 12, 53115 Bonn,
E-mail: quadt@physik.uni-bonn.de

Abstract:
The precise measurement of the proton structure function $F_2(x, Q^2)$ in a wide x- and Q^2-range in deep inelastic ep scattering at HERA has been and continues to be one of the most exciting and instructive tests of perturbative QCD. An overview of the highlights of such analyses, in particular in H1 and ZEUS†, is given here.

1. Introduction

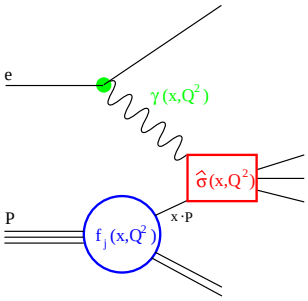

Figure 1: Schematic factorisation diagram of DIS events with the three contributions to the calculation.

Deep inelastic lepton nucleon scattering (DIS) experiments have played a crucial rôle in the understanding of hadronic matter. They have revealed the structure of hadrons as to consist of constituents (quarks and gluons) interacting according to Quantum Chromodynamics (QCD). HERA offers the possibility to study the structure of the proton with a resolution of about 10^{-18} m, three orders of magnitude smaller than the proton itself.

The kinematics of the deep inelastic scattering process, $e + p \to e + X$, can be completely described by the negative four-momentum transfer squared, Q^2, which is inversely proportional to the square of the transverse resolution power, and Bjorken x, which can be interpreted as the fraction of the proton momentum carried by the struck quark. For convenience, the relative energy transfer in the proton rest frame, y, is also introduced, yielding, together with the ep center-of-mass energy squared, s, the relation $Q^2 = s \cdot x \cdot y$.

The schematic factorisation diagram of lepton-proton scattering in figure 1 shows the three contributions which enter the cross section calculation of a particular DIS process:

$$\sigma = \gamma(x, Q^2) \otimes f_i(x, Q^2) \otimes \hat{\sigma}(x, Q^2), \tag{1.1}$$

*Speaker.

†This report mainly presents ZEUS results in which the speaker was directly involved. Similar results have been published by the H1 collaboration.

where $\gamma(x,Q^2)$ contains the electroweak flux and couplings of the exchanged γ, Z^0 or $W^\pm$ bosons, and $f_i(x,Q^2)$ describes the distribution of partons of flavour i and proton momentum fraction x in the proton when probed at a scale Q^2. Finally, $\hat{\sigma}(x,Q^2)$ denotes the hard parton boson cross section of the reaction considered, which can be calculated in perturbative QCD (pQCD). The study of such processes allows tests of the proton structure and QCD. The main questions are:

- Parton dynamics, i.e. does DGLAP of pQCD describe the evolution of parton densities in x, Q^2 ?
- How low in Q^2 can one go before perturbative QCD breaks down ?
- Are the parton density functions *universal* ? Can they be extracted from measurements of one process and be used to successfully describe some other process when inserted into the pQCD calculation ?
- If yes, hard cross section calculations can also be tested and the strong coupling α_s can be extracted.

2. Early F_2 - Measurements at HERA

At HERA, collisions between 27.5 GeV electrons[1] and 820 GeV protons extend the accessible kinematic range in x and Q^2 by 2-3 orders of magnitude compared to previous fixed-target experiments (see figure 2).

The double-differential neutral current cross section for inclusive $e^\pm p$ scattering is given in terms of the structure functions F_i:

$$\frac{d^2\sigma(e^\pm p)}{dx\,dQ^2} = \frac{2\pi\alpha^2}{xQ^4}\left[Y_+\,F_2(x,Q^2) \mp Y_- xF_3(x,Q^2) - y^2 F_L(x,Q^2)\right]\cdot\left(1+\delta_r(x,Q^2)\right) \quad (2.1)$$

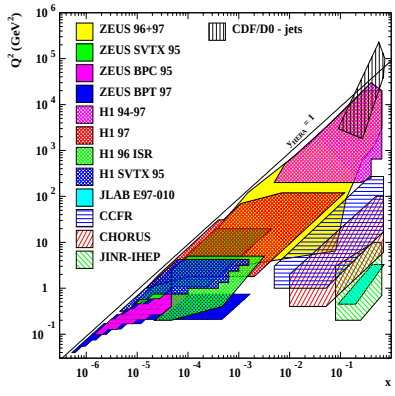

Figure 2: Extended kinematic plane coverage by HERA.

where $Y_\pm = 1 \pm (1-y)^2$ and x and Q^2 are defined at the hadronic vertex. In this equation, F_L is the longitudinal structure function, xF_3 is the parity-violating term arising from Z^0 exchange and δ_r is the electroweak radiative correction. The structure function F_2 contains contributions from both virtual photon and Z^0 exchange:

$$F_2 = F_2^{em} + \frac{Q^2}{(Q^2+M_Z^2)}F_2^{int} + \frac{Q^4}{(Q^2+M_Z^2)^2}F_2^{wk} \quad (2.2)$$

where M_Z is the mass of the Z^0 and the contribution to F_2 from photon exchange (F_2^{em}), Z^0 exchange (F_2^{wk}) and the $Z^0-\gamma$ interference term (F_2^{int}) are separately indicated. At Q^2 well below M_Z, F_2 is dominated by F_2^{em}, where[2] $F_2^{em}(x,Q^2) = \sum_f e_f^2\cdot(xq_f + x\bar{q_f})$, the sum of quark- and antiquark momentum distributions weighted by the charge squared. The fixed-target F_2 data reach down only to x of $\sim 10^{-2}$, i.e. stay essentially in the valence regime and leave considerable uncertainty in the gluon-dominated low-x parton densities.

[1] 1994-1997 positrons were used for the lepton beam. 'Electron' is used as a generic term for the scattered lepton. From 1998 onwards the proton beam energy was 920 GeV.

[2] at LO or in the DIS renormalisation scheme

Using about $500\,\mathrm{nb}^{-1}$ of electron-proton data, recorded in 1993, H1 and ZEUS measured the steep rise in F_2 towards low x values of $10^{-4} - 10^{-2}$ in the range $Q^2 = 8.5 - 2000\,\mathrm{GeV}^2$ with 10% - 20% precision[3] (see figure 3) [1]. This steep rise in F_2 was quite surprising and is attributed to the large gluon density in the proton at low x and the increased gluon splitting into $q\bar{q}$-pairs, followed by further gluon radiation of the latter (parton cascade). It is a consequence of the parton dynamics in the proton; in constrast, a hadron-like behaviour would result in a flat $F_2(x)$. After this observation, the low-x regime became of growing interest for the following reasons: (1) The large event statistics at low Q^2 allows precision measurements of cross-sections and F_2, allowing for stringent QCD tests and the extraction of parton density functions. (2) As the low-x parton dynamics are dominated by the gluon, precise cross-section measurements allowed the determination of the hitherto unknown gluon density. Precise knowledge of the latter would, in turn, allow additional stringent tests of QCD predictions. (3) It is this low-x, low-Q^2 regime where deviations in the parton evolution from the DGLAP-behaviour due to parton- (gluon)-recombination, saturation or other effects and a breakdown of perturbative QCD are first expected to show up.

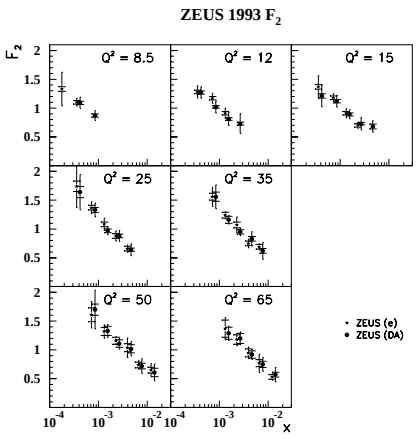

Figure 3: F_2 as a function of x as measured by ZEUS using the 1993 data.

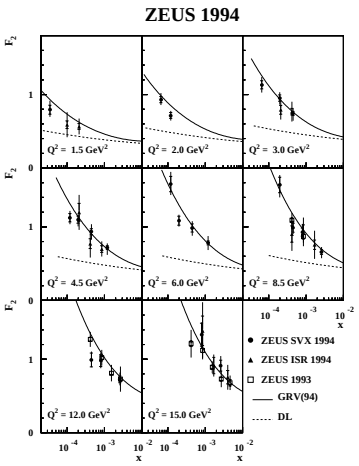

Figure 4: F_2 as a function of x as measured by ZEUS using the 1994 data.

The experimental reach down to low Q^2 is limited by the detector acceptance in the direction of the scattered electron. Using the 1993 data, H1 and ZEUS have already studied ways to increase the low-Q^2 acceptance, by (a) reducing the hole in the calorimeter for the beampipe and improved measurement of the energy and angle of the scattered electron; (a) selecting events with a tagged hard initial-state photon radiation (ISR), resulting in lower Q^2 for a given electron energy and scattering angle; and (c) selecting events from the proton satellites, which occur delayed by $\sim 2.5\,\mathrm{ns}$, i.e. shifted by $\sim 70\,\mathrm{cm}$ away from the detecting calorimeter. Option (c) lead in 1994 to so-called 'shifted-vertex runs (SVX)', i.e. runs where HERA was tuned such that the majority of ep collisions occured shifted by $\sim 70\,\mathrm{cm}$ along the beamline with respect to the nominal interaction point.

[3] H1 extended the measurement down to $Q^2 \approx 4.5\,\mathrm{GeV}^2$ using the proton satellite events.

Using these techniques and $58\,\mathrm{nb}^{-1}$ of data for the SVX-analysis and $2.5\,\mathrm{pb}^{-1}$ for the ISR-analysis resulted in the measurement of $F_2(x, Q^2)$ down to $Q^2 = 1.5\,\mathrm{GeV}^2$ with 10% - 30% precision [2]. The surprising result (see figure 4) was that F_2 is still rising at such low Q^2 values and that this behaviour can be well described by pQCD calculations as shown here by the GRV-model[3]. This celebrated success of pQCD was unexpected and created the desire to go to even lower Q^2 and map out the entire transition region from the DIS regime to real photoproduction at $Q^2 = 0\,\mathrm{GeV}^2$.

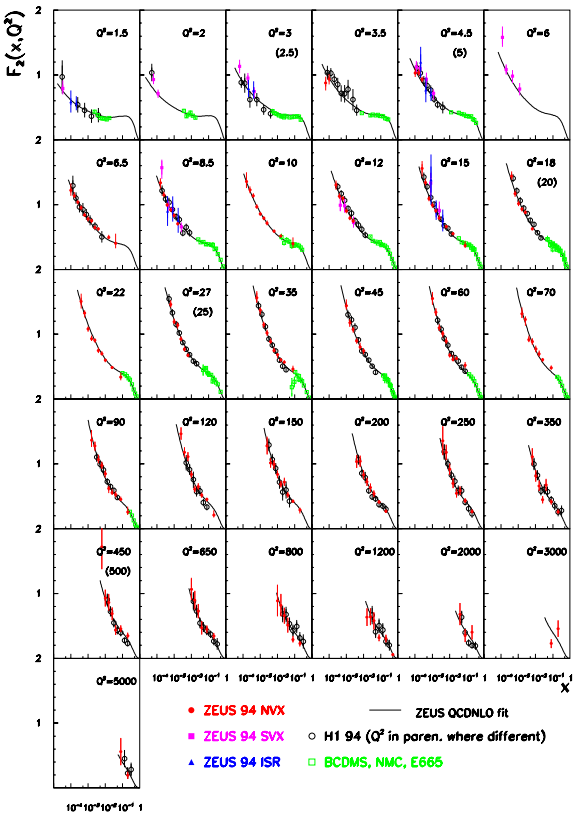

Figure 5: Summary of F_2 as function of x as measured by H1 and ZEUS using the 1994 data.

In addition to these special analyses, the HERA experiments also performed F_2 measurements from the full 1994 data sample of $2.5\,\mathrm{pb}^{-1}$ [4]. Due to improved detector understanding, increased detector acceptance and sophisticated kinematic reconstruction techniques, exploiting the over-constrained system of the electron and the visible hadronic final state, the measurements reached a typical precision of 4% - 5% ($Q^2 < 100\,\mathrm{GeV}^2$) and covered the kinematic range of $3 \cdot 10^{-5} - 0.5$ in x and $3.5 - 5000\,\mathrm{GeV}^2$ in Q^2. The combined results showed, good agreement between the two HERA experiments, and revealed the sharp rise in F_2 at low x, precisely measured in this large kinematic range and smoothly connecting to the fixed-target data. This data set provided, for a long time, the reference data for numerous phenomenological studies, QCD tests and the extraction of parton densities and α_s for the experiments as well as global QCD analyses.

ZEUS, for example, performed a next-to-leading order (NLO) QCD fit to the F_2 data from ZEUS (also including low-Q^2 data from 1995), NMC and BCDMS by parametrising the parton density functions at the starting scale $Q_0^2 = 7\,\mathrm{GeV}^2$, evolving them up to high Q^2 using the DGLAP-evolution equations and minimising the global χ^2 of the resulting calculated F_2 to the measured data points [5]. In this procedure, the charm and bottom contribution, F_2^c, F_2^b were calculated in NLO using massive splitting functions where $\alpha_s(M_Z^2) = 0.118$ was assumed as input to the fit. This fit can describe the measured F_2 data points pretty well (see figure 5) and allows the extraction of the gluon momentum density with 10% precision at $Q^2 = 20\,\mathrm{GeV}^2$ (see figure 6). At such large Q^2 values, the gluon density is much larger than the quark-(singlet) density, so that the gluons drive the evolution of the sea quarks. At $Q^2 = 7\,\mathrm{GeV}^2$ this gluon dominance decreases and turns, at $Q^2 = 1\,\mathrm{GeV}^2$, into a roughly flat gluon density whereas the sea-quark density is still rising towards low x (figure 6). This observation, that the sea

quarks appear to drive the evolution of the gluon density at low Q^2, can be interpreted as being close to the limit of validity of pQCD.

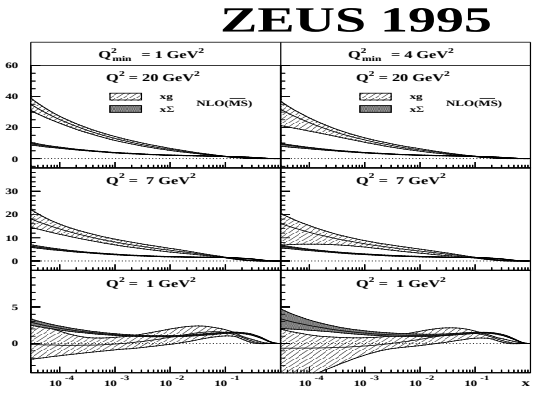

Figure 6: Gluon and sea-quark density as a function of x as extracted from the ZEUS QCD fit.

3. Low x- and Q^2-Analyses

In order to cover the detector acceptance gap between the DIS regime of a few GeV^2 in Q^2 and photoproduction ($Q^2 = 0\,\mathrm{GeV}^2$), ZEUS installed in 1995 a small electromagnetic calorimeter (the 'beam pipe calorimeter') with good energy and position resolution around the beampipe. This device extended the ZEUS acceptance down to $Q^2 = 0.1\,\mathrm{GeV}^2$, allowing the desired measurements of the virtual photon-proton scattering cross section or F_2 in the transition region [6].

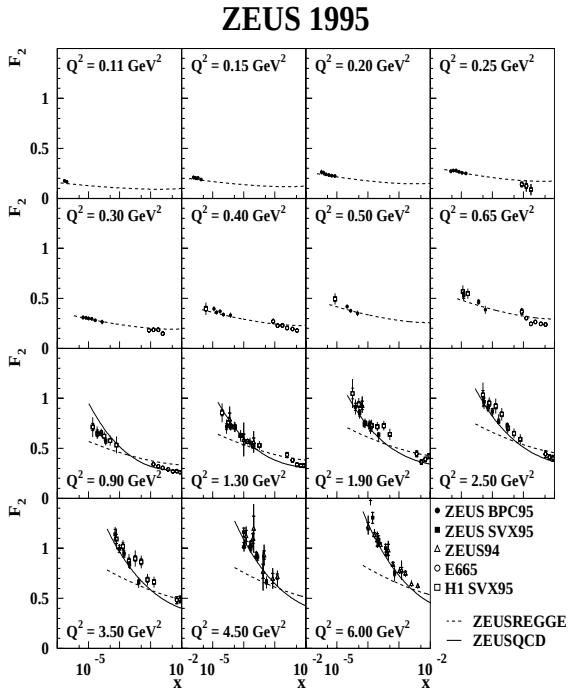

Figure 7: Low Q^2 $F_2(x)$ in the transition region, in combination with the afore mentioned data.

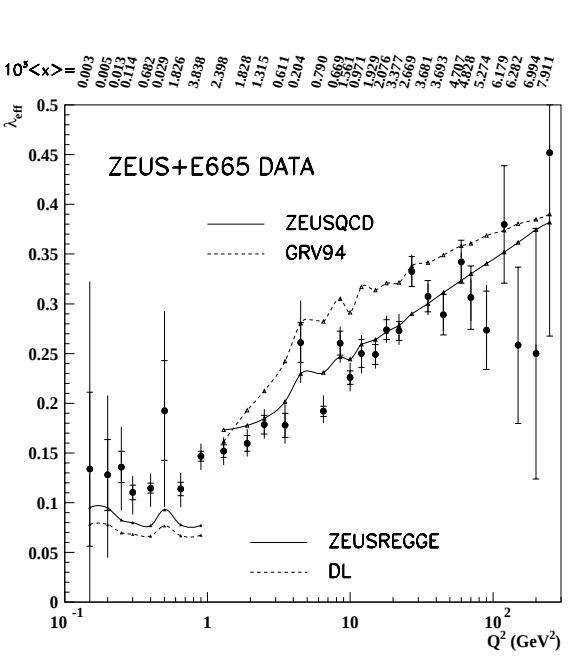

Figure 8: $\lambda_{eff} = d\ln F_2/d\ln(1/x)$ as a function of Q^2.

Figure 7 shows the resulting F_2 as a function of x for $Q^2 = 0.11 - 6.0\,\mathrm{GeV}^2$. At the highest Q^2, F_2 still exhibits the steep rise towards low x and can be described by pQCD. However, for Q^2 below $\approx 0.65\,\mathrm{GeV}^2$, F_2 becomes rather flat and cannot be described by pQCD anymore, whereas a Regge-inspired fit does describe this hadronic behaviour of the

proton. Fitting the F_2 data to a functional form of $A\,x^{-\lambda_{eff}}$ for $x < 10^{-2}$ allows the steepness of the rise in F_2 and its change in the Q^2 range of 0.11 - 300 GeV^2 (figure 8) [5] to be quantified. This Q^2 dependence of the F_2 slope can also be well described by pQCD above $Q^2 \approx 1\,\mathrm{GeV}^2$ whereas below that region the F_2 slope stays essentially constant at about the value of 0.08 - 0.11, also known as the soft pomeron slope for total hadronic cross sections.

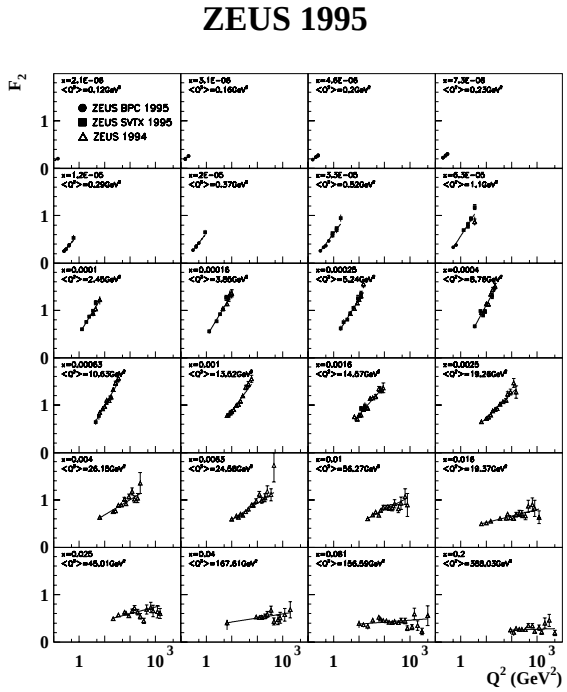

Figure 9: $F_2(Q^2)$ in x bins.

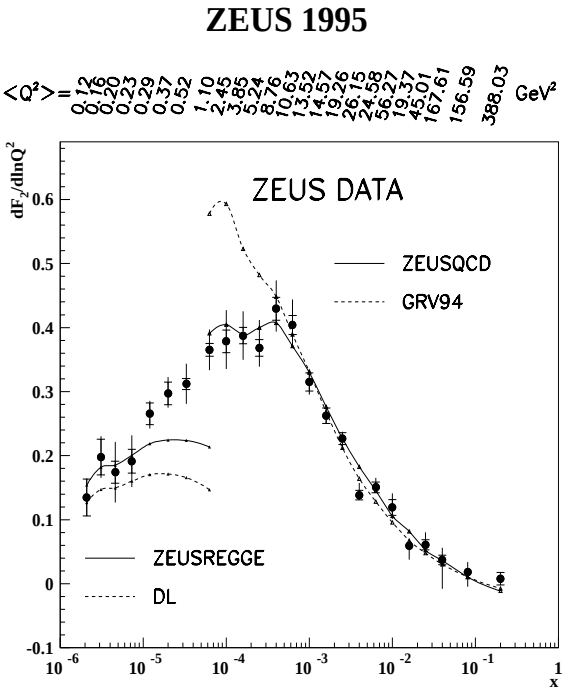

Figure 10: $dF_2/d\ln Q^2$ as a function of x.

Similarly the scaling violations of F_2 were investigated. Figure 9 shows the F_2 data as a function of Q^2 for fixed values of x. At large Q^2, F_2 is reasonably flat, an observation which led in the 60s to the conclusion that a proton consists of three spin-$\frac{1}{2}$ constituents, the quarks. At low x, however, strong scaling violations are observed, a result of the gluon splitting. The strength of this effect is quantified by fitting the functional form $F_2 = a + b\,\ln Q^2$, where $b \sim \alpha_s\, P_{qg} \otimes g(x)$ with the gluon-quark splitting function P_{qg} and the gluon density $g(x)$. Figure 10 shows the dependence of the slope $dF_2/d\ln Q^2$ with increasing x (and Q^2). The comparison of the slope values with the model points, obtained in identical ways, indicate that pQCD can describe well the Q^2 slopes in the data from large x and Q^2 down to $Q^2 \approx 1\,\mathrm{GeV}^2$, whereas at lower x and Q^2 the Regge-inspired models provide a better description of the data. The observation that at $Q^2 \approx 1 - 8\,\mathrm{GeV}^2$ the Q^2 slope flattens off while the x-slopes become constant, but non-zero is qualitatively consistent with the results of the QCD fit, i.e. the flat behaviour of the gluon density while the sea quark distribution is still steep at low x. Further interpretations of these results, particularly in the context of possible low-x, low-Q^2 saturation effects are difficult as the measurements are at the edge of the accessible phase space. Further discussions and interpretations are still ongoing, for example in these proceedings [7].

4. Precision Measurements of F_2

After this first phase of structure function and cross section measurements at HERA, the focus shifted towards precision measurements of these quantities. ZEUS measured the neutral current cross section $\frac{d\sigma^{NC}}{dx}$ and $\frac{d\sigma^{NC}}{dQ^2}$ at high Q^2 using $47.7\,\mathrm{pb}^{-1}$ of e^+p data [8]. The subset of $30.6\,\mathrm{pb}^{-1}$ from 1996-97 has been used for an F_2 measurement above $Q^2 \approx 30\,\mathrm{GeV}^2$ and a $2.2\,\mathrm{pb}^{-1}$ for a measurement at $Q^2 > 2\,\mathrm{GeV}^2$, amounting to 0.56 and 1.3 million events, respectively [9]. Since these large data samples result in small statistical errors, the main challenge has been the control and reduction of systematic uncertainties. Possible detector resolution and efficiency effects, the Monte Carlo modelling, trigger uncertainties, kinematic reconstruction techniques etc. have been very carefully studied. In the high Q^2 regime one of the most exciting measurements is that of the differential neutral current cross section. Earlier preliminary results had indicated an excess of events at very high Q^2 and x while the final analysis of the complete e^+p data shows very good agreement between the data and the Standard Model prediction, except, maybe, the last bin around Q^2 of $\sim 40\,000\,\mathrm{GeV}^2$ (see figure 11). In particular, the dependence on the γ- or Z^0-virtuality is very well reproduced, showing no sign of new physics. Similarly, the x-differential cross section result (figure 12) is very well reproduced by the Standard Model calculation, indicating that the parton densities, particularly $xu(x)$, are well modelled and have rather small uncertainties (yellow bands). In further studies, the sensitivity to the neutral current propagator $\frac{Q^2}{Q^2+M_Z^2}$ and hence to the mass of the Z^0 has been demonstrated, providing first results of electroweak measurements at HERA.

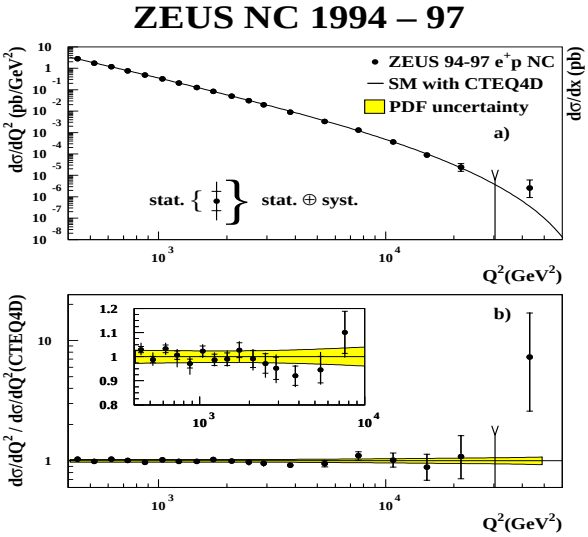

Figure 11: High Q^2 neutral current cross section $d\sigma/dQ^2$.

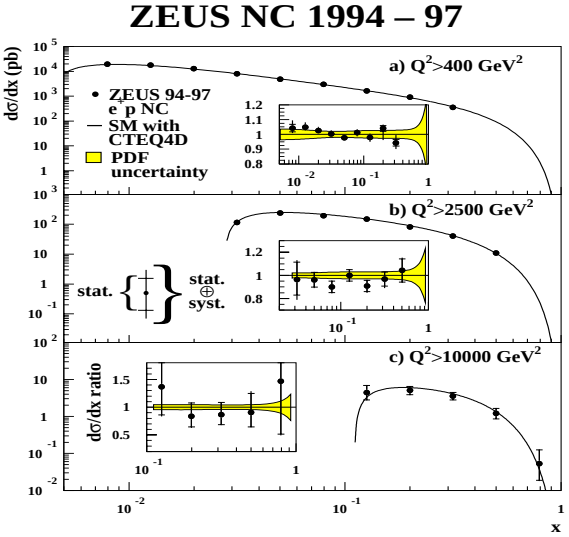

Figure 12: High Q^2 neutral current cross section $d\sigma/dx$.

The double differential neutral current cross section or $F_2(x, Q^2)$ measurement using this data set is statistics limited only above $Q^2 > 800 - 1000\,\mathrm{GeV}^2$. At medium and low Q^2 the statistical errors are $\sim 1\%$ and the systematic uncertainties typically $2 - 4\%$. The precision of this measurement is therefore twice as good as the previous one using the 1994

data and reaches the fixed-target level. Figure 13 shows the resulting $F_2(x)$ at typical Q^2 values in comparison to the 1994 measurement, the fixed-target data and three different QCD fits. The new measurement is consistent with the previous one, but covers a larger x, Q^2-range with reduced errors and better resolution. Also the new data can be very well described by the ZEUS QCD fit whereas the spread of the global QCD analyses (MRST99 and CTEQ5D [11]) is indicates the uncertainty band of the earlier data. Consequently, global QCD analyses including the new measurements will reduce the uncertainty in the quark and even more in the gluon density functions, allowing in turn even more stringent QCD tests in the production of exclusive final states and the determination of α_s.

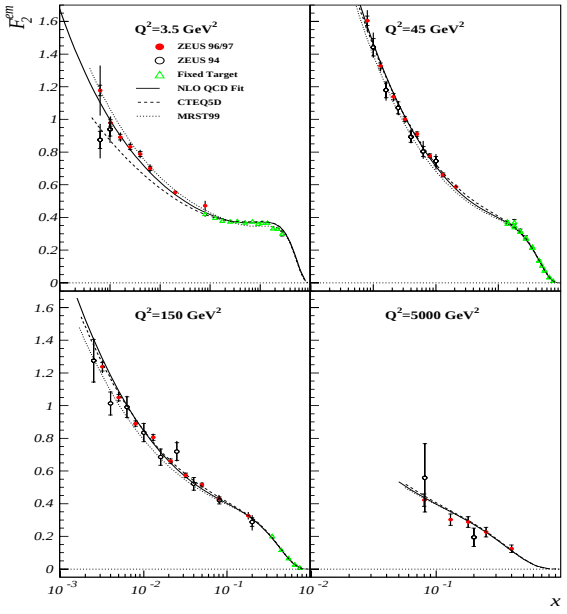

Figure 13: $F_2(x)$ at typical Q^2 values.

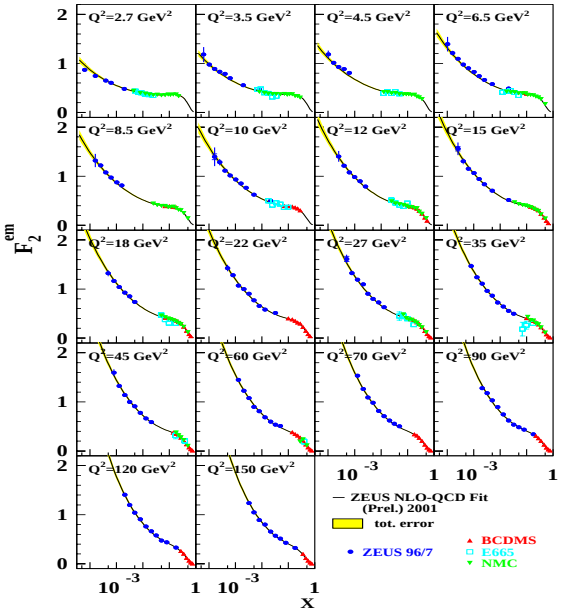

Figure 14: Overview of the ZEUS $F_2(x)$ with fixed-target data.

An overview of the latest F_2 results as a function of x for different Q^2 values is given in figure 14. The F_2 data connects smoothly to the fixed-target data and exhibits similar precision in a large x, Q^2-range. The scaling violations of $F_2(Q^2)$ are summarised in figures 15 and 16.

5. Towards the lowest x and Q^2

The installation of the ZEUS beam-pipe tracker, a silicon-strip telescope with angular resolution of $\sigma_\Theta = 0.2\,\text{mrad}$, an efficiency known to better than 1.5% and a relative alignment with respect to the beam-pipe calorimeter (BPC) to better than $200\,\mu\text{m}$ allowed the reduction of the BPC energy-scale uncertainty and non-uniformity and hence provided a further opportunity for very low-Q^2 measurements of F_2. In the extreme kinematic range down to $Q^2 = 0.045\,\text{GeV}^2$ and $6 \cdot 10^{-7} < x < 1 \cdot 10^{-3}$, F_2 could be measured with statistical and systematic precision of 2.5% and 3.3%, respectively [10]. The resulting F_2 as a function of x is shown in figure 17 down to the lowest Q^2. In the lowest Q^2 range, the data exhibits very

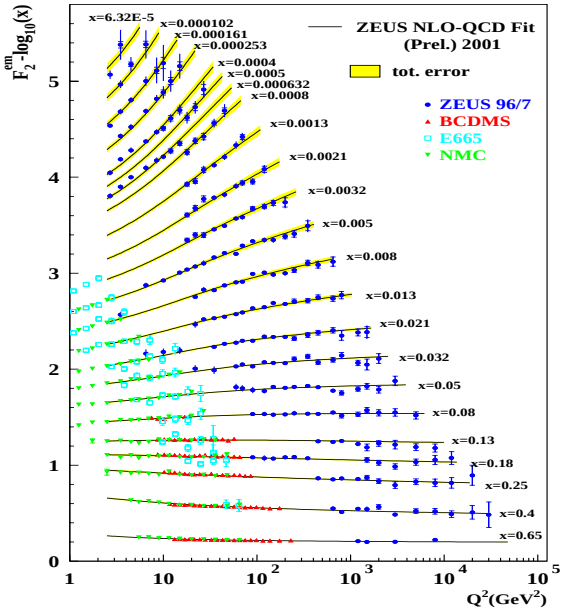

Figure 15: F_2 scaling violations overview.

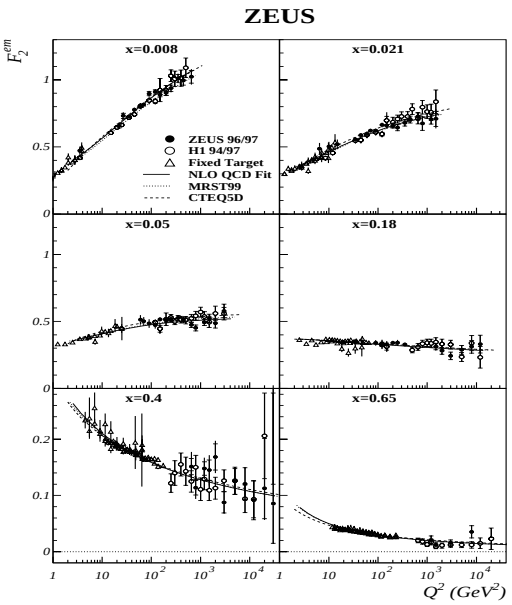

Figure 16: $F_2(Q^2)$ at typical x values.

clearly a flat, hadron-like behaviour and can be well described by a Regge-motivated fit. In figure 18, F_2 can be seen as a function of Q^2 for fixed values of y or W^2. The transition region towards the $Q^2 = 0\,\mathrm{GeV}^2$ photoproduction is mapped out and F_2 vanishes like Q^2 for $Q^2 \to 0$, as expected. This analysis provides a wealth of data for ongoing phenomenological studies of the transition region, possible saturation effects and the breakdown of pQCD.

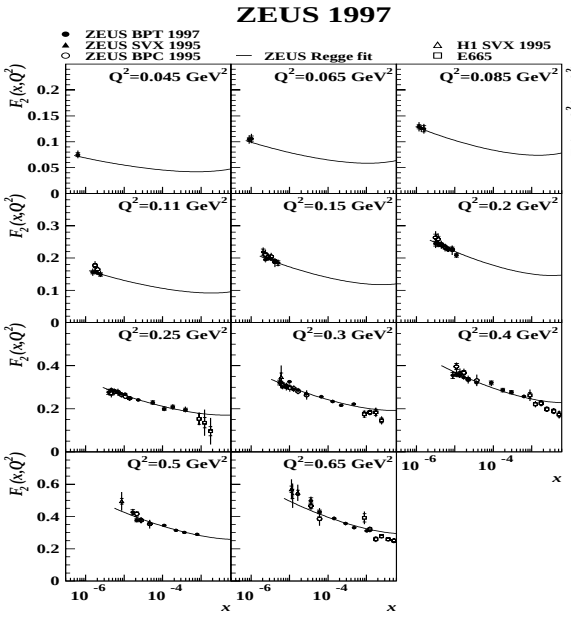

Figure 17: $F_2(x)$ at lowest Q^2 values.

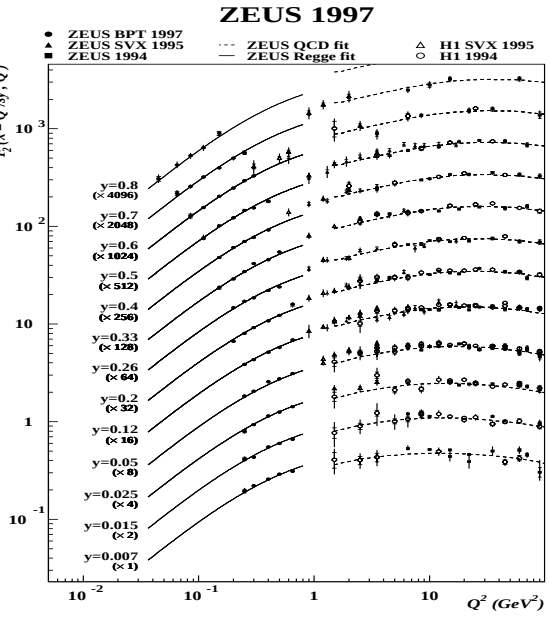

Figure 18: $F_2(Q^2)$ in the transition region.

6. Summary and Outlook

Over the last few years precise measurements of the neutral and charged current inclusive cross sections and the proton structure function F_2 were performed with increasing x, Q^2 coverage. This, together with further studies of exclusive processes, allowed numerous QCD tests along with the extraction of parton density functions and α_s. These measurements provided an improved quantitative understanding of the proton structure and QCD.

The analysis of more HERA data is also expected to provide exciting results on other structure functions such as xF_3, F_L and to allow further phenomenological studies and data interpretations, in both the very low-Q^2 and the high-Q^2 regime.

The start of the upgraded HERA-II in the fall 2001 is the onset of a new era of HERA physics, aiming at an improved understanding of the flavour decomposition of F_2, exciting electroweak measurements and the search for new physics. The increased luminosity as well as the polarised electron beam will play important rôles in this program.

Acknowledgements

I am grateful to the EPS and feel very honoured to have been awarded the *'Young Particle Physicist Prize'*. Experimental high energy physics today is only possible in large international collaborations. Consequently, I did all my research with many people from all over the world, whom I wish to thank heartily for the collaboration, help, support and the wonderful time we had. Special thanks go to my colleagues and friends in Oxford, the ZEUS-UK group, the H1 and ZEUS collaborations and to DESY.

References

[1] ZEUS Collaboration, M. Derrick et al., *Z. Physik* **C 65** (1995) 379.

[2] ZEUS Collaboration, M. Derrick et al., *Z. Physik* **C 69** (1996) 4.

[3] M. Glück, E. Reya und A. Vogt, *Z. Physik* **C 53** (1992) 127; M. Glück, E. Reya und A. Vogt, *Phys. Lett.* **B 306** (1993) 391; M. Glück, E. Reya und A. Vogt, *Z. Physik* **C 67** (1995) 433.

[4] ZEUS Collaboration, M. Derrick et al., *Z. Physik* **C 72** (1996) 3.

[5] ZEUS Collaboration, J. Breitweg et al., *Eur. Phys. J.* **C 7** (1999) 609.

[6] ZEUS Collaboration, J. Breitweg et al., *Phys. Lett.* **B 407** (1997) 432.

[7] A. Gotsman and H. Kowalski in Proceedings of the EPS International Conference on High Energy Physics, Budapest, 2001 (D. Horvath, P. Levai, A. Patkos, eds.), JHEP (http://jhep.sissa.it/) Proceedings Section, PrHEP-hep2001/053, PrHEP-hep2001/054; 'The dipole picture of small x physics: A SUMMARY OF THE AMIRIM MEETING.' M.F. McDermott, DESY-00-126, hep-ph/0008260.

[8] ZEUS Collaboration, J. Breitweg et al., *Eur. Phys. J.* **C 11** (1999) 3.

[9] ZEUS Collaboration, S. Chekanov et al., *Eur. Phys. J.* **C 21** (2001) 3.

[10] ZEUS Collaboration, J. Breitweg et al., *Phys. Lett.* **B 487** (2000) 1.

[11] CTEQ Collab., H.L. Lai et al., *Eur. Phys. J.* **C 12** (2000) 375; A.D. Martin et al. [MRST], *Eur. Phys. J.* **C 14** (2000) 133.